

Dinitrogen Complexes

Dinitrogen Coordination to a High-Spin Diiron(I/II) Species

Juan F. Torres, Collin H. Oi, Ian P. Moseley, Nabila El-Sakkout, Brian J. Knight, Jason Shearer,* Ricardo García-Serres,* Joseph M. Zdrozny,* and Leslie J. Murray*

Abstract: Dinitrogen coordination to iron centers underpins industrial and biological fixation in the Haber–Bosch process and by the FeM cofactors in the nitrogenase enzymes. The latter employ local high-spin metal centers; however, iron–dinitrogen coordination chemistry remains dominated by low-valent states, contrasting the enzyme systems. Here, we report a high-spin mixed-valent *cis*-(μ -1,2-dinitrogen)diiron(I/II) complex $[(\text{FeBr})_2(\mu\text{-N}_2)\text{L}^{\text{bis}}]^-$ (**2**), where $[\text{L}^{\text{bis}}]^-$ is a bis(β -diketiminato) cyclophane. Field-applied Mössbauer spectra, dc and ac magnetic susceptibility measurements, and computational methods support a delocalized $S = 7/2$ Fe_2N_2 unit with $D = -5.23 \text{ cm}^{-1}$ and consequent slow magnetic relaxation.

Converting atmospheric dinitrogen into bioavailable forms (e.g., NH_3) is essential to life on Earth. However, scission of dinitrogen is a kinetically-limited reaction.^[1] The Haber–Bosch process for industrial production of NH_3 employs the iron-based Mittasch catalyst and high temperatures and pressures to achieve reductive cleavage of N_2 .^[2] Contrastingly, nitrogenase enzymes in biological systems effect N_2 reduction to NH_3 under ambient conditions utilizing Fe_7M (M=Mo, V or Fe) cofactors with local high-spin Fe centers.^[3] Whereas iron reactive sites in the Mittasch catalyst are predominantly in reduced states,^[2] the nitrogenase cofactors are proposed to employ a cluster with minimal, if any, low valent iron character for N_2 conversion to NH_3 .^[4–7]

However, N_2 coordination to high-spin Fe centers remains dominated by low valent states.^[1] Motivated by these observations, we explored reduction of a diiron(II) complex supported by a dinucleating cyclophane in the presence of dinitrogen, resulting in the most oxidized dinitrogen-bridged iron complex with local high spin centers to date. This complex also displays the *cis*- μ -1,2 coordination mode, which remains rare in diiron chemistry with only two other examples reported (Figure 1). Notably, prior examples were obtained for highly-reduced compounds or using strong-field ligands contrasting the ligand field imposed here.^[8,9]

Previously, trinuclear $3d$ metal complexes of a tris(β -diketiminato) cyclophane ($\text{H}_3\text{L}^{\text{Eu/Me}}$) were shown competent for N_2 activation.^[10–12] Analogous to the synthesis of $\text{H}_3\text{L}^{\text{Eu/Me}}$, Schiff base condensation of 1,3-bis(aminomethyl)-2,4,6-triethylbenzene with the monoketal of acetylacetonone affords $\text{H}_2\text{L}^{\text{bis}}$ (Scheme S2), which can be deprotonated and metalated with FeBr_2 to give $\text{Fe}_2\text{Br}_2\text{L}^{\text{bis}}$ (**1**) (92% yield). The solid-state structure of **1** is analogous to reported (di-halido)diiron(II) cores and the $\text{Fe}_2(\mu_3\text{-Br})(\mu\text{-Br})$ fragment of $\text{Fe}_3\text{Br}_3\text{L}^{\text{Eu/Me}}$ (Figure S17).^[13] Complex **1** is distinct from previous reports, however, in the dihedral angle of $150.6(1)^\circ$ between the β -diketiminato (or BDI) planes, which is more acute than analogous aggregates of mononuclear metal complexes.

Reaction of $\text{Fe}_2\text{Br}_2\text{L}^{\text{bis}}$ with 1 equiv of $[\text{K}(\text{18-crown-6})(\text{THF})_2](\text{C}_{10}\text{H}_8)$ in THF at -35°C under Ar affords a green solution that decomposes over several hours at low temperature. Attempts to crystallize this species were unsuccessful, yielding red crystals of the formally diiron(II)

[*] J. F. Torres, C. H. Oi, B. J. Knight, L. J. Murray
 Center for Catalysis and Florida Center for Heterocyclic Chemistry,
 Department of Chemistry
 University of Florida
 Gainesville, FL 32611 (USA)
 E-mail: murray@chem.ufl.edu

I. P. Moseley, J. M. Zdrozny
 Department of Chemistry, Colorado State University
 Fort Collins, CO 80523 (USA)
 E-mail: Joe.Zdrozny@colostate.edu

N. El-Sakkout, R. García-Serres
 Univ. Grenoble Alpes, CNRS, CEA, IRIG, Laboratoire de Chimie et
 Biologie des Métaux
 17 rue des Martyrs, 38000 Grenoble (France)
 E-mail: ricardo.garcia@cea.fr

J. Shearer
 Department of Chemistry, Trinity University
 San Antonio, TX 78212 (USA)
 E-mail: jshearer@trinity.edu

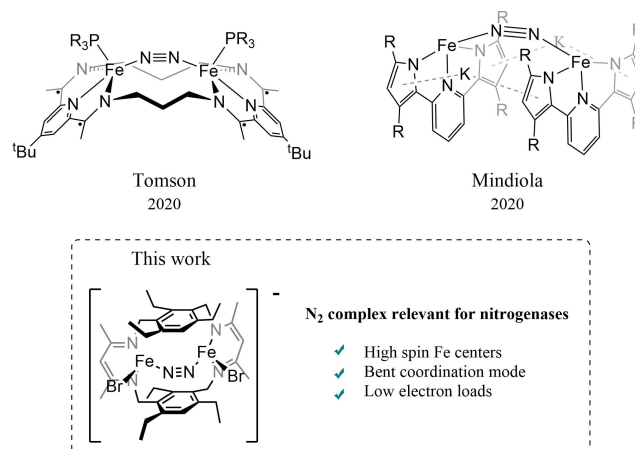
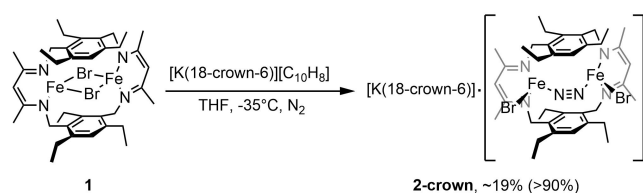


Figure 1. Reported *cis*-(μ -1,2-dinitrogen)diiron complexes.

complex $[(\text{FeBr})_2(\mu\text{-Br})\text{L}^{\text{bis}}]^- (\text{Br}_3)$ (Figure S18). In situ reaction of the reduced green species with dinitrogen rapidly afford the dark red compound $[\text{K}(18\text{-crown-6})(\text{THF})_2][(\text{FeBr})_2(\mu\text{-N}_2)\text{L}^{\text{bis}}]$ (**2-crown**) in excellent yield ($>90\%$ by ^1H NMR), albeit only 19% was isolated as crystalline solid. The N–N stretching mode at 1932 cm^{-1} shifts to 1870 cm^{-1} when $^{15}\text{N}_2$ is used, consistent with the predicted value (1866 cm^{-1}) and confirming N_2 incorporation (Figure S11). Comparable results were obtained when complex **1** was reduced at -35°C under a N_2 atmosphere (Scheme 1). Compound **2-crown** decomposes above 40°C and under reduced pressure, presumably from N_2 dissociation based on loss of the assigned N–N stretching mode in IR spectra.

Despite numerous attempts, we were only able to determine a connectivity structure of **2-crown** by single-crystal X-ray diffraction (SCXRD) (Figure S19). Employing $[\text{K}(\text{crypt-222})][\text{C}_{10}\text{H}_8]$ as the reductant, however, yields **2-crypt** of which single crystals of sufficient quality for a structure solution by SCXRD could be grown. The $[(\text{FeBr})_2(\mu\text{-N}_2)\text{L}^{\text{bis}}]^-$ complex ion is isostructural in **2-crown** and **2-crypt** with no apparent effect of the non-interacting counter-cation, based on the connectivity structure solutions (Figure S21), IR spectra (Figures S10 and S12), paramagnetic ^1H NMR spectra (Figures S4 and S6), and calculated solution magnetic moments ($\mu_{\text{eff}}=7.64\ \mu_{\text{B}}$ and $7.77\ \mu_{\text{B}}$ for **2-crown** and **2-crypt**, respectively). Each Fe center in **2-crypt** resides in a pseudo-tetrahedral coordination environment with τ_4 values of 0.94 and 0.93 for Fe1 and Fe2, respectively (*viz.* $\tau_4=1$ for tetrahedral).^[14] The dinitrogen ligand in **2-**



Scheme 1. Reaction scheme for synthesis of complex **2-crown**. Yield evaluated by ^1H NMR in parenthesis.

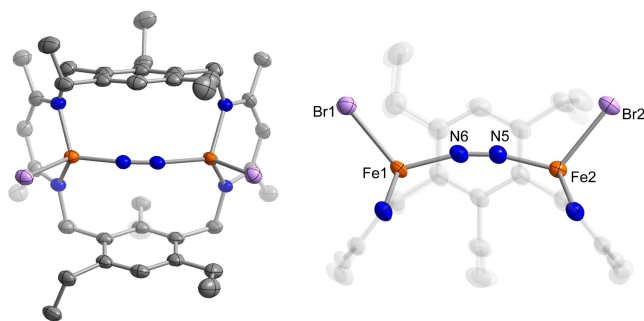


Figure 2. Crystal structure of the anion $[(\text{FeBr})_2(\mu\text{-N}_2)\text{L}^{\text{bis}}]^-$ from complex **2-crypt** with the thermal ellipsoids at the 65% probability level (left). All H atoms are omitted for clarity. C, N, Br, and Fe atoms depicted as gray, blue, pink, and orange ellipsoids, respectively. Core of $[(\text{FeBr})_2(\mu\text{-N}_2)\text{L}^{\text{bis}}]^-$ anion from **2-crypt** (right). Selected bond lengths [Å]: Fe1–Fe2 4.7562(4), N5–N6 1.164(6). Selected angles [°]: Fe1–N6–N5 164.8(2), Fe2–N5–N6 167.0(2).

crypt adopts a *cis*- μ -1,2 mode with Fe–N–N angles of 167.0(2) and 164.8(2) (Figure 2). The diiron core undergoes substantial structural rearrangement from **1** to **2** (*viz.* $\Delta d_{\text{Fe-Fe}} > 1\ \text{Å}$, Figure S28). Notably, **2-crypt** has a longer Fe–Fe distance (4.7562(4) Å) than one predicted for the observed Fe–N–N bond angle based on structures reported (Figure S22).

Few mixed-valent dinitrogen-bridged iron complexes have been characterized,^[15–18] with **2** being the most oxidized to date. The zero-applied field 80-K Mössbauer spectrum of **2-crown** displays a single quadrupole doublet, implying valence delocalization across both iron centers (Figure 3a). The isomer shift for the metal centers in **2-crown** ($\delta=0.81\text{ mm s}^{-1}$) is comparable to those observed for tetrahedral high-spin Fe^{II} BDI complexes, with only a slight decrease with respect to **1** ($\delta_1=0.86\text{ mm s}^{-1}$ and $\delta_1=0.90\text{ mm s}^{-1}$, Figure S25). Variable temperature Mössbauer spectra (Figure S26) reveal slow relaxation behavior with intermediate relaxation behavior from 8–20 K and features from the fast and slow relaxation limits persist throughout the swept temperature range (2.35 K to 30 K). Applied-field spectra below 8 K or above 20 K were simulated as composites of fast- and slow-relaxing fractions calculated with the same $S=7/2$ spin Hamiltonian (Figure 3b). Simulations of data recorded between 5.8 and 35 K provide estimates for the zero-field splitting parameters of $D=-5\text{ cm}^{-1}(\pm 1\text{ cm}^{-1})$ and $0.2 < E/D < 1/3$ (Figure S27). These values are in good agreement with those determined from magnetic susceptibility measurements (see below and Table S2).

Variable-temperature direct-current (dc) magnetic susceptibility ($\chi_{\text{M}}T$) measurements corroborate the ground-state spin observed for **2-crown** in the Mössbauer data (Figure 3c). At room temperature, the value of $\chi_{\text{M}}T$ is $8.12\text{ cm}^3\text{ K mol}^{-1}$, which remains relatively constant with decreasing temperature to 50 K. The $\chi_{\text{M}}T$ value at room temperature compares well with the effective moment measured by Evans method and that expected for an $S=7/2$ system ($7.85\text{ cm}^3\text{ K mol}^{-1}$, $g=2.00$) rather than weakly coupled $S=2\text{ Fe}^{\text{II}}$ and $S=3/2\text{ Fe}^{\text{I}}$ ions ($\approx 4.9\text{ cm}^3\text{ K mol}^{-1}$ with $g=2.00$).^[19] Below 50 K, $\chi_{\text{M}}T$ values decrease rapidly to $5.83\text{ cm}^3\text{ K mol}^{-1}$ at 5 K due to zero-field splitting. Modeling this temperature dependence of $\chi_{\text{M}}T$ yields best fit values consistent with a rhombic $S=7/2$ system of $g_x=2.05$, $g_y=2.10$, $g_z=1.97$, and zero-field splitting terms of $D=-5.23\text{ cm}^{-1}$ and $|E|=1.53\text{ cm}^{-1}$ (see Supporting Information for additional fitting details). The magnitude of D is in the expected range for N_2 bridged dinuclear weak-field ligated Fe complexes.^[17]

Alternating current susceptibility measurements of **2-crown** at zero-applied field reveal a frequency-dependent out-of-phase ac susceptibility (χ_{M}'') signal near 11 Hz below 6.0 K (Figure 3c inset, S24). Applying a static magnetic field shifts the peaks to lower frequency, evidencing a slowing of the magnetic relaxation process and possible disruption of a contribution from a tunneling relaxation mechanism.^[20] Relaxation times (τ) determined with a Debye model support Arrhenius-like behavior with an effective activation energy for relaxation (U_{eff}) of 16.3 cm^{-1} and an attempt time of $1.9 \times 10^{-6}\text{ s}$ (Figure S23).^[21] Although the limited temper-

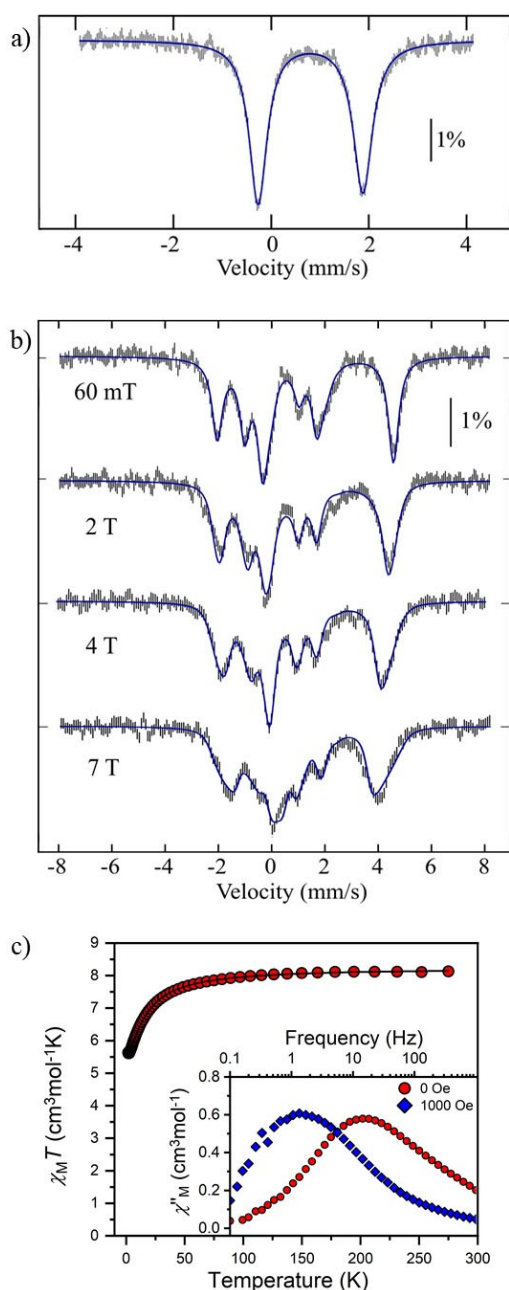


Figure 3. a) Zero-field Mössbauer spectrum of **2-crown** recorded at 80 K. The solid line represents a simulation with $\delta = 0.81 \text{ mm s}^{-1}$, $\Delta E_Q = 2.14 \text{ mm s}^{-1}$, and $\Gamma = 0.44/0.48 \text{ mm s}^{-1}$. b) Mössbauer spectra of **2-crown** recorded at 2.35 K (top spectrum) or 5.8 K in variable magnetic fields applied parallel to the direction of the gamma-rays. The simulation (solid lines) was performed assuming only one iron site in the slow relaxation limit, with admixture of 18% of the absorbers in the fast relaxation limit. Fitting parameters are given in table S3. c) Variable-temperature, dc susceptibility data for **2-crown** taken under a 1000 Oe applied field. The black line is the best fit obtained, full fitting details can be found in the Supporting Information. (inset) Ac susceptibility data measured at 1.8 K under zero applied field (red) and a 1000 Oe applied field (blue).

ature range investigated here prevents conclusive assignment of the relaxation processes present, these observations show slow magnetization dynamics arising from a negative

D parameter, consistent with the $\chi_M T$ and Mössbauer data.^[20]

Turning to DFT calculations, the geometry optimized structure of $[(\text{FeBr})_2(\mu\text{-N}_2)\text{L}^{\text{bis}}]^-$ using BP86/def2-tzvp with Grimme's D3 dispersion correction and $S = 7/2$ ground state agrees with the crystallographic data for **2-crypt** and **2-crown**, including the *cis*- μ -1,2 coordination mode of the dinitrogen ligand (Table S4). Vibrational analysis (B2PLYP/def2-tzvp) yields an N–N stretching frequency of 1944.7 cm^{-1} , which agrees with the experimental values of 1932 cm^{-1} . Similarly, calculated Mössbauer parameters of $\delta_{\text{calc}} = 0.81 \text{ mm s}^{-1}$ and $\Delta E_{Q,\text{calc}} = 2.76 \text{ mm s}^{-1}$ are in excellent agreement with the experimental values (*viz.* $\delta_{\text{exp}} = 0.81 \text{ mm s}^{-1}$ and $\Delta E_{Q,\text{exp}} = 2.14 \text{ mm s}^{-1}$). The calculated zero-field splitting parameters reproduce the negative value of D and $E/D \approx 0.3$; however, the magnitudes of the zero-field splitting parameters were approximately twice that derived from the Mössbauer and magnetic susceptibility data. From the B2PLYP/def2-tzvp/CP(PPP) calculations, the seven singly occupied orbitals are predominantly Fe $3d$ in character with Fe $3d$ compositions ranging from 78–98% (Figure S29). The extent of activation of the N_2 ligand is readily reflected in the presence of only one frontier molecular orbital of appreciable Fe d_π to $\text{N}_2 \pi^*$, which is predominantly $\text{N}_2 \pi^*$ in character.

The electronic structure of **2** differs from the three-spin model and the ferromagnetically coupled metal centers model commonly used to explain the magnetic properties of M–N₂–M fragments.^[22] The absence of significant unpaired-spin contribution on the N₂ ligand suggests that the observed delocalization is likely mediated by a double-exchange mechanism analogous to that reported for mixed-valent divanadium complexes.^[23] Electron delocalization across a neutral bridging dinitrogen was previously proposed to explain the magnetic properties of a covalent μ -1,2-N₂ dicobalt(I) BDI complex.^[24] Complex **2** demonstrate that *cis*-dinitrogen bridged iron complexes can display valence delocalization (Figure S28), affording Mössbauer parameters nearly indistinguishable from formal iron(II) centers, and suggest that such reduced state can be present in the enzymes cofactors.

In conclusion, we report the synthesis and characterization of the first $S = 7/2$ mixed-valent *cis*-(μ -1,2-dinitrogen)diiron(I/II) complex. The observed N₂-coordination mode remains rare for μ -N₂-dirion complexes due to the expected decrease in π -backbonding vs. a linear mode. Here, $[\text{L}^{\text{bis}}]^{2-}$ limits the accessible dihedral angles between the two BDI planes resulting in the preferred bent mode. This compound demonstrates that polynuclear Fe species are competent to bind N₂ with electron loadings, formal oxidation states, local spin states, and coordination modes feasible for the nitrogenase enzyme system.

Acknowledgements

Authors thank Dr. S. N. MacMillan and A. L. Rheingold for the XRD measurements and the National Institutes of Health (R01-GM123241: J.F.T., C.H.O., B.J.K., L.J.M.),

Labex ARCANE and CBH-EUR-GS (ANR-17-EURE-0003: N.E.S., R.G.S.), National Science Foundation (CHE-1854854: J.S.), and the National Science Foundation Graduate Research Fellowship Program (006784-00002: I.P.M., J.M.Z.).

Conflict of Interest

The authors declare no conflict of interest.

Data Availability Statement

The data that support the findings of this study are available in the Supporting Information of this article.

Keywords: Electronic Structure · Mixed-Valent Compounds · Multiiron Complexes · Nitrogen Fixation

-
- [1] D. Singh, W. R. Buratto, J. F. Torres, L. J. Murray, *Chem. Rev.* **2020**, *120*, 5517–5581.
- [2] G. Ertl, *Angew. Chem. Int. Ed.* **2008**, *47*, 3524–3535; *Angew. Chem.* **2008**, *120*, 3578–3590.
- [3] L. C. Seefeldt, Z.-Y. Yang, D. A. Lukoyanov, D. F. Harris, D. R. Dean, S. Raugei, B. M. Hoffman, *Chem. Rev.* **2020**, *120*, 5082–5106.
- [4] Z.-Y. Yang, N. Khadka, D. Lukoyanov, B. M. Hoffman, D. R. Dean, L. C. Seefeldt, *Proc. Natl. Acad. Sci. USA* **2013**, *110*, 16327–16332.
- [5] A. T. Thorhallsson, B. Benediktsson, R. Bjornsson, *Chem. Sci.* **2019**, *10*, 11110–11124.
- [6] D. A. Lukoyanov, Z.-Y. Yang, D. R. Dean, L. C. Seefeldt, S. Raugei, B. M. Hoffman, *J. Am. Chem. Soc.* **2020**, *142*, 21679–21690.
- [7] M. Rohde, D. Sippel, C. Trncik, S. L. A. Andrade, O. Einsle, *Biochemistry* **2018**, *57*, 5497–5504.
- [8] T. Liu, M. R. Gau, N. C. Tomson, *J. Am. Chem. Soc.* **2020**, *142*, 8142–8146.
- [9] D. Sorsche, M. E. Miehlich, K. Searles, G. Gouget, E. M. Zolnhofer, S. Fortier, C.-H. Chen, M. Gau, P. J. Carroll, C. B. Murray, K. G. Caulton, M. M. Khusniyarov, K. Meyer, D. J. Mindiola, *J. Am. Chem. Soc.* **2020**, *142*, 8147–8159.
- [10] Y. Lee, F. T. Sloane, G. Blondin, K. A. Abboud, R. García-Serres, L. J. Murray, *Angew. Chem. Int. Ed.* **2015**, *54*, 1499–1503; *Angew. Chem.* **2015**, *127*, 1519–1523.
- [11] R. B. Ferreira, B. J. Cook, B. J. Knight, V. J. Catalano, R. García-Serres, L. J. Murray, *ACS Catal.* **2018**, *8*, 7208–7212.
- [12] M. C. Eaton, B. J. Knight, V. J. Catalano, L. J. Murray, *Eur. J. Inorg. Chem.* **2020**, 1519–1524.
- [13] G. L. Guillet, F. T. Sloane, D. M. Ermert, M. W. Calkins, M. K. Pephrah, E. S. Knowles, E. Čížmár, K. A. Abboud, M. W. Meisel, L. J. Murray, *Chem. Commun.* **2013**, *49*, 6635–6637.
- [14] L. Yang, D. R. Powell, R. P. Houser, *Dalton Trans.* **2007**, 955–964.
- [15] K. Grubel, W. W. Brennessel, B. Q. Mercado, P. L. Holland, *J. Am. Chem. Soc.* **2014**, *136*, 16807–16816.
- [16] L. D. Field, R. W. Guest, P. Turner, *Inorg. Chem.* **2010**, *49*, 9086–9093.
- [17] S. F. McWilliams, P. C. Bunting, V. Kathiresan, B. Q. Mercado, B. M. Hoffman, J. R. Long, P. L. Holland, *Chem. Commun.* **2018**, *54*, 13339–13342.
- [18] T. A. Betley, J. C. Peters, *J. Am. Chem. Soc.* **2003**, *125*, 10782–10783.
- [19] D. F. Evans, *J. Chem. Soc.* **1959**, 2003–2005.
- [20] C. E. Jackson, I. P. Moseley, R. Martinez, S. Sung, J. M. Zadrozny, *Chem. Soc. Rev.* **2021**, *50*, 6684–6699.
- [21] P. Debye, *Ann. Phys.* **1912**, *344*, 789–839.
- [22] P. L. Holland, *Dalton Trans.* **2010**, *39*, 5415–5425.
- [23] B. Bechlars, D. M. D'Alessandro, D. M. Jenkins, A. T. Iavarone, S. D. Glover, C. P. Kubiak, J. R. Long, *Nat. Chem.* **2010**, *2*, 362–368.
- [24] K. Ding, A. W. Pierpont, W. W. Brennessel, G. Lukat-Rodgers, K. R. Rodgers, T. R. Cundari, E. Bill, P. L. Holland, *J. Am. Chem. Soc.* **2009**, *131*, 9471–9472.
- [25] Deposition Numbers 2121401 (for **1**), 2121402 (for **Br₃**), 2121403 (for **2-crypt**), and 2121404 (for H₂L^{bis}) contain the supplementary crystallographic data for this paper. These data are provided free of charge by the joint Cambridge Crystallographic Data Centre and Fachinformationszentrum Karlsruhe Access Structures service.

Manuscript received: February 14, 2022

Accepted manuscript online: March 18, 2022

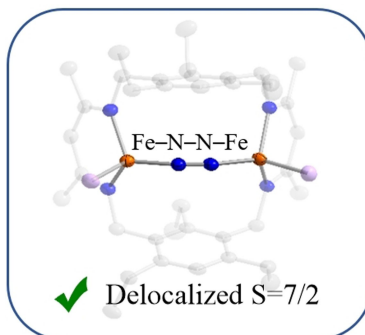
Version of record online: ■■■, ■■■

Communications

Dinitrogen Complexes

J. F. Torres, C. H. Oi, I. P. Moseley, N. El-Sakkout, B. J. Knight, J. Shearer,* R. García-Serres,* J. M. Zadrozny,*
L. J. Murray* _____ e202202329

Dinitrogen Coordination to a High-Spin
Diiron(I/II) Species



Dinitrogen coordination to multiiron complexes is instrumental in understanding the reactivity of nitrogenases cofactors. The synthesis of a high-spin mixed-valent *cis*-(μ -1,2-dinitrogen)diiron(I/II) complex obtained by a one-electron reduction of a diiron(II/II) precursor is reported. The electronic structure of the complex was studied using Mössbauer spectroscopy, SQUID magnetometry, and DFT calculations, which support a $S=7/2$ ground state.